Design and Implementation of a Lithography Chamber Environment Controller Based on Decoupling of Temperature and Humidity

Hongjing Yang [1], Jiao Yang [1, *], Guangbo Li [1], Xucheng Li [1], Dayang Ren [2]

[1]School of Electrical and Engineering, Liaoning Institute of Science and Technology, Benxi, Liaoning 117004, China

[2]Shenyang Field Technology Co., Ltd. Shenyang, Liaoning, 110000, China

Abstract

Lithography, as the cornerstone of semiconductor manufacturing, imposes stringent tolerances on the temperature and humidity of the exposure chamber. However, the strong coupling between these two variables makes conventional PID control inadequate. To address this issue, we propose a decoupling-oriented environmental controller for the lithography chamber. First, by analyzing the internal heat- and mass-transfer mechanisms, a two-input/two-output transfer-function model of the chamber is established. A feedforward compensator is then designed to generate pre-feedback decoupling signals, which are further refined by a Hebb-rule neural-network decoupler to actively cancel cross-interference between the temperature and humidity loops. The hardware is built around an STM32F407 microcontroller and integrates auxiliary heating, refrigeration, and humidification modules. The software architecture comprises a main scheduler, data-acquisition service, and environmental-factor control kernels. Experimental results show that the controller maintains the chamber temperature within 23 ± 0.13 °C and relative humidity between 54 % RH and 57 % RH, satisfying the accuracy and dynamic-response requirements of mainstream lithographic processes.

Keywords

Temperature and Humidity Decoupling; Environmental Control; Feedforward Compensation; Hebb Neural Network.

1. INTRODUCTION

In recent years, with the rise of emerging technologies such as artificial intelligence, 5G communication, and the Internet of Things, the demand for semiconductors has continued to grow [1]. The semiconductor industry, as the core of modern technology, has a profound impact on the global economy and technological progress. Lithography is one of the most critical steps in semiconductor manufacturing. Its main function is to precisely transfer the designed circuit patterns onto the semiconductor substrate [2]. This process is achieved through the use of photoresist and lithography machines. The photoresist undergoes a chemical reaction under the illumination of light at a specific wavelength, thereby forming the desired pattern. The accuracy of the lithography process directly determines the minimum feature size of semiconductor devices, which in turn affects the performance, power consumption, and integration level of chips. At present, most mainstream lithography machine environment control systems adopt an independent closed-loop control structure based on the PID algorithm. However, this approach ignores the inherent strong coupling relationship between the two key

ISSN: 2472-3703 DOI: 10.6911/WSRJ.202511_11(11).0009

physical quantities of temperature and humidity. During the temperature and humidity control process, when cooling and dehumidifying the air, a decrease in temperature will cause an increase in relative humidity; while using the heating method to reduce relative humidity, it will cause temperature fluctuations. This coupling effect makes the traditional single-loop PID control highly susceptible to "seesaw" oscillations, with large system overshoot and long settling time, making it difficult to meet the stringent requirements for control accuracy (such as temperature ±0.1°C, humidity ±1% RH) and dynamic response of high-order processes [2]. To address the above problems, this paper proposes an advanced control scheme based on the idea of temperature and humidity decoupling [3]. By establishing an accurate system coupling model and designing a decoupling algorithm that combines feedforward compensation and dynamic matrix control, the mutual interference between the temperature and humidity loops is actively canceled in theory and structure, thereby achieving independent, precise, and rapid stable control of the two controlled quantities.

2. REQUIREMENTS FOR TEMPERATURE AND HUMIDITY ENVIRONMENT INSIDE THE LITHOGRAPHY CHAMBER

2.1. Requirements for Temperature Control

The optical systems (such as lens groups and mirrors) and mechanical structures (such as guide rails and frames) of a lithography machine are manufactured using specific materials (like ultra-low expansion glass, ceramics, and invar). However, even with materials possessing extremely low coefficients of thermal expansion, minute temperature variations (e.g. ±0.1°C) can still induce nanometer-scale deformations [4]. Such deformations directly alter optical path lengths and lens curvatures, causing the imaging focal plane to drift and aberrations to increase, ultimately leading to pattern distortion and a decline in resolution. Modern lithography requires the overlaying of multiple patterns. Non-uniform thermal expansion of the wafer and reticle due to temperature gradients during the exposure process directly causes misalignment between layers. This error cannot be fully compensated through software calibration and represents a fundamental physical bottleneck limiting overlay accuracy.

Therefore, temperature control within the lithography machine chamber is extremely stringent. For advanced processes (such as EUV lithography), the internal chamber temperature typically needs to be stabilized at 23±0.1°C or even tighter, and spatial temperature gradients throughout the chamber must also be minimized to ensure thermal field uniformity.

2.2. Requirements for Humidity Control

Fluctuations in the water vapor content in the air (humidity) directly alter the specific heat capacity and thermal conductivity of the air. In precision temperature control systems, humidity variations are equivalent to introducing a dynamic thermal load, which interferes with the control loops of high-precision air conditioning systems and indirectly leads to temperature instability. The photoresist in photolithography machines is hygroscopic. Changes in humidity cause these materials to absorb or release moisture, resulting in micro-expansion or contraction, which affects their dimensional stability and mechanical properties, potentially introducing minor alignment or leveling errors [5]. If humidity is not properly controlled, there may be a risk of micro-condensation on surfaces with lower temperatures. Water molecules can adsorb onto optical components and wafer surfaces, not only altering their optical properties but also reacting with residual hydrocarbons in a vacuum environment to form a contaminant layer, severely reducing the reflectivity and lifespan of optical components.

Based on the above mechanisms, the humidity inside the photolithography chamber typically needs to be controlled within a narrow range of 35% to 45% relative humidity, with fluctuations

ISSN: 2472-3703 DOI: 10.6911/WSRJ.202511_11(11).0009

less than ±1%. In special applications such as EUV lithography, the control precision of humidity and the dew point temperature requirements are even stricter.

3. ANALYSIS AND ESTABLISHMENT OF THE CHAMBER ENVIRONMENT CONTROL MODEL

In the photolithography machine chamber, heat conduction, convection, and radiation are the main modes of heat transfer that affect the distribution of temperature and humidity. Heat conduction refers to the transfer of heat through the vibration of molecules within a material, convection refers to the transfer of heat through the movement of fluids, and radiation refers to the transfer of heat through electromagnetic waves. Specifically, heat conduction and convection cause changes in the temperature gradient within the chamber, thereby affecting the saturation of water vapor in the air [6]. When the temperature gradient is large, the diffusion rate of water vapor increases, leading to an uneven distribution of humidity. Radiation affects the humidity distribution indirectly by changing the temperature of the chamber surfaces. Therefore, the coupling relationship between temperature and humidity can be described through heat transfer equations. In control theory, the mathematical model of the system can be described using a transfer function. This paper uses the data experimental method to calibrate the time response curves of temperature and humidity for the entire system, and obtains the transfer function of the system based on the time response curves:

$$H(s) = \frac{Y(s)}{X(s)} = \frac{C}{Ts+k} e^{s} \tag{1}$$

Where T is the system time constant, is the system gain, and is the system constant.

Since the control objectives of the system studied in this paper are temperature and humidity, the system is a dual-input and dual-output system. The system transfer function $H(s)$ can be described as a matrix of temperature and humidity:

$$\begin{bmatrix} TEMP \\ HUM \end{bmatrix} = \begin{bmatrix} H_{temp-temp}(s) & H_{hum-temp}(s) \\ H_{temp-hum}(s) & H_{thum-hum}(s) \end{bmatrix} \begin{bmatrix} \Delta TEMP \\ \Delta HUM \end{bmatrix} \tag{2}$$

Where $H_{temp-temp}(s)$ is the transfer function for temperature control, $H_{hum-temp}(s)$ is the transfer function of humidity on temperature, $H_{temp-hum}(s)$ is the transfer function of temperature control on humidity, and $H_{hum-hum}(s)$ is the transfer function of humidity on humidity. Thus, the following can be obtained:

$$TEMP = H_{temp-temp}(s) \times \Delta TEMP + H_{hum-temp}(s) \times \Delta HUM \tag{3}$$

$$HUM = H_{temp-hum}(s) \times \Delta TEMP + H_{thum-hum}(s) \times \Delta HUM \tag{4}$$

4. DECOUPLER DESIGN

4.1. Feedforward Signal Decoupler

If the effects of humidity changes on temperature and temperature changes on humidity are removed, the temperature and humidity control in the photolithography chamber can be transformed from a dual-input and dual-output system to a single-input and single-output system. This can improve the accuracy of temperature and humidity control in the photolithography chamber and reduce the control complexity. In this paper, the system is

ISSN: 2472-3703 DOI: 10.6911/WSRJ.202511_11(11).0009

modified using decoupling methods, introducing the temperature decoupling transfer function $H_{decoup-temp}(s)$ and the humidity decoupling transfer function $H_{decoup-hump}(s)$.

In the field of control, diagonal matrix method, feedforward compensation method, and identity matrix method are widely used in decoupling control. Among them, the identity matrix method requires high implementation standards, while the diagonal matrix method and feedforward compensation method have similar decoupling effects. However, the feedforward decoupling method has a simpler network structure and better stability and efficiency, making it the most widely used decoupling method [7]. The decoupling structure can be located either before the control signal or between the control signal and the controlled signal. If the decoupling algorithm is placed before the control signal, the system solution becomes more complex[8]. In this system, the decoupling algorithm is located between the controller and the controlled object, as shown in the following mathematical equation:

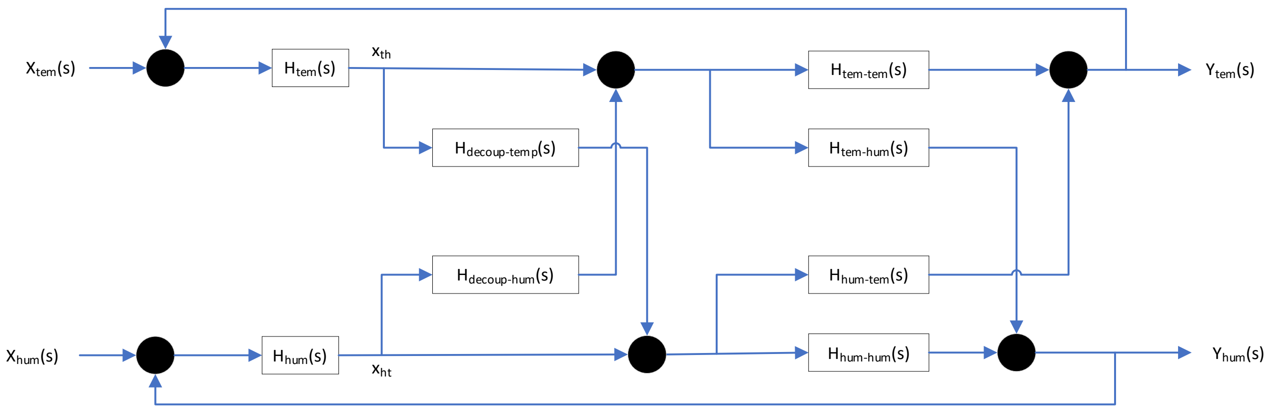

Figure 1. Feedback Compensation Temperature and Humidity Control Structure Diagram

In the decoupled system, let

$$\Delta HUM \times H_{hum-temp}(s) + \Delta HUM \times H_{decoup-hump}(s) \times H_{temp-temp}(s) = 0 \quad (5)$$

In the decoupled system, let Obtain the decoupling formula

$$H_{decoup-hump}(s) = -\frac{H_{hum-temp}(s)}{H_{temp-temp}(s)} \quad (6)$$

let

$$EMP \times H_{temp-hum}(s) + \Delta TEMP \times H_{decoup-temp}(s) \times H_{hump-hump}(s) = 0 \quad (7)$$

In the decoupled system, let Obtain the decoupling formula

$$H_{decoup-hump}(s) = -\frac{H_{temp-hum}(s)}{H_{hum-hum}(s)} \quad (8)$$

Substituting Equation (6) and Equation (8) yields the transfer function $H_d(S)$ of the decoupling network compensator.

$$H_d(S) = \begin{bmatrix} 1 & H_{decoup-hump}(s) \\ H_{decoup-hump}(s) & 1 \end{bmatrix} = \begin{bmatrix} 1 & -\frac{H_{hum-temp}(s)}{H_{temp-temp}(s)} \\ -\frac{H_{temp-hum}(s)}{H_{hum-hum}(s)} & 1 \end{bmatrix} \quad (9)$$

ISSN: 2472-3703 DOI: 10.6911/WSRJ.202511_11(11).0009

By incorporating the transfer function $H_d(S)$ of the decoupling network compensator into the temperature and humidity control structure, the strongly coupled temperature and humidity system is transformed into a single-input and single-output system with interrelated characteristics, thereby achieving decoupling of the system's temperature and humidity.

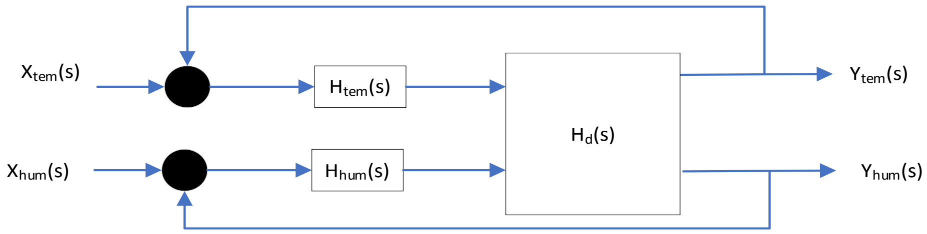

Figure 2. Decoupled Temperature and Humidity Control Structure for the Greenhouse

4.2. Decoupler Based on Hebbian Neural Network

Artificial neural networks are essentially a simulation of biological neural networks [9]. Hebbian learning is a type of learning rule in neural networks. In 1949, Hebb proposed an unsupervised learning rule to explain and describe the learning process. This rule suggests that when one neuron repeatedly participates in the activity of another, the connection strength between these two neurons will be enhanced. This principle is considered fundamental to synaptic reinforcement in the brain and is often used to explain certain phenomena observed during neural network learning. Its mathematical expression is given in.

$$\Delta\omega_{ij}(k) = \eta O_i(k) O_j(k) \tag{10}$$

O_i and O_j denote the outputs of neurons i and j, respectively, and $\Delta\omega_{ij}(k)$ represent the change in the connection weight between the two neurons; η is the learning rate [9].

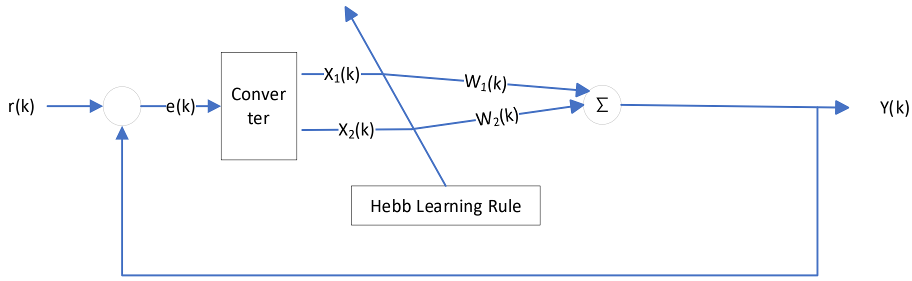

Figure 3. Principle of Neuron PD Control

The system can be expressed in the form of Fig. 3 by means of the neural network, where r(k) denotes the set-point, e(k) the error, and y(k) the output; the above-mentioned system is accordingly described as

$$\begin{aligned} \omega_1(k) &= \omega_1(k-1) + \eta_P e(k) x_1(k) \\ \omega_2(k) &= \omega_2(k-1) + \eta_I e(k) x_2(k) \end{aligned} \tag{11}$$

η_P denotes the proportional learning rate, and η_I the integral learning rate; this arrangement enables more efficient adjustment of the individual weight coefficients. A larger η_P yields smaller overshoot but slower convergence, whereas a larger η_I produces greater overshoot yet faster convergence.

ISSN: 2472-3703 DOI: 10.6911/WSRJ.202511_11(11).0009

5. SYSTEM IMPLEMENTATION AND TEST RESULTS

5.1. System Hardware Framework

The system consists of a main controller, a touch screen (human-machine interface), auxiliary heating equipment (heating pipes), cooling equipment (air conditioning system), a humidification system (humidifier), a lighting system (adjustable brightness cold LED lights), and a ventilation system (combined ventilation fans), as shown in Figure 4.

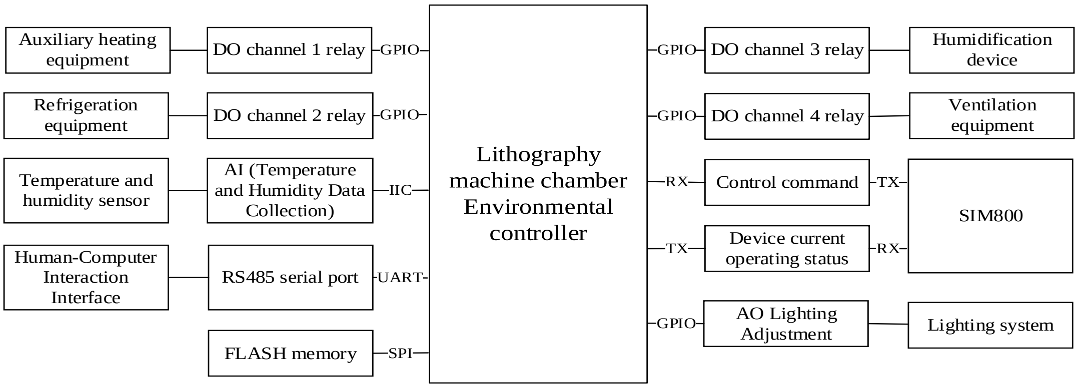

Figure 4. chematic diagram of the environmental controller inside the lithography machine chamber

The main chip of the environmental controller inside the lithography machine chamber is the STM32F407 microcontroller. The microprocessor controls the start and stop of auxiliary heating, refrigeration, humidification, and ventilation equipment through 4 digital outputs. It adjusts the brightness of the lighting system via 1 analog output. Communication with the touchscreen is achieved through an RS485 serial interface, allowing operators to set control segments and parameters via the touchscreen. Communication with the remote control center is handled by the SIM800 module. The FLASH memory is used to store temperature setting parameters for the lithography machine's chamber, as well as the key parameters of the pre-feedback decoupling algorithm and the single-neuron PD algorithm. In the early training phase, the single-neuron PD learning algorithm is completed on a remote server; afterward, the trained parameters and algorithm are flashed into the FLASH memory.

5.2. Software Design

The overall software design is shown in Figure 5 and mainly consists of seven parts: the main scheduling module, software initialization module, runtime parameter configuration module, Alibaba Cloud data transmission module, remote control module, manual control module, and automatic operation module.

ISSN: 2472-3703 DOI: 10.6911/WSRJ.202511_11(11).0009

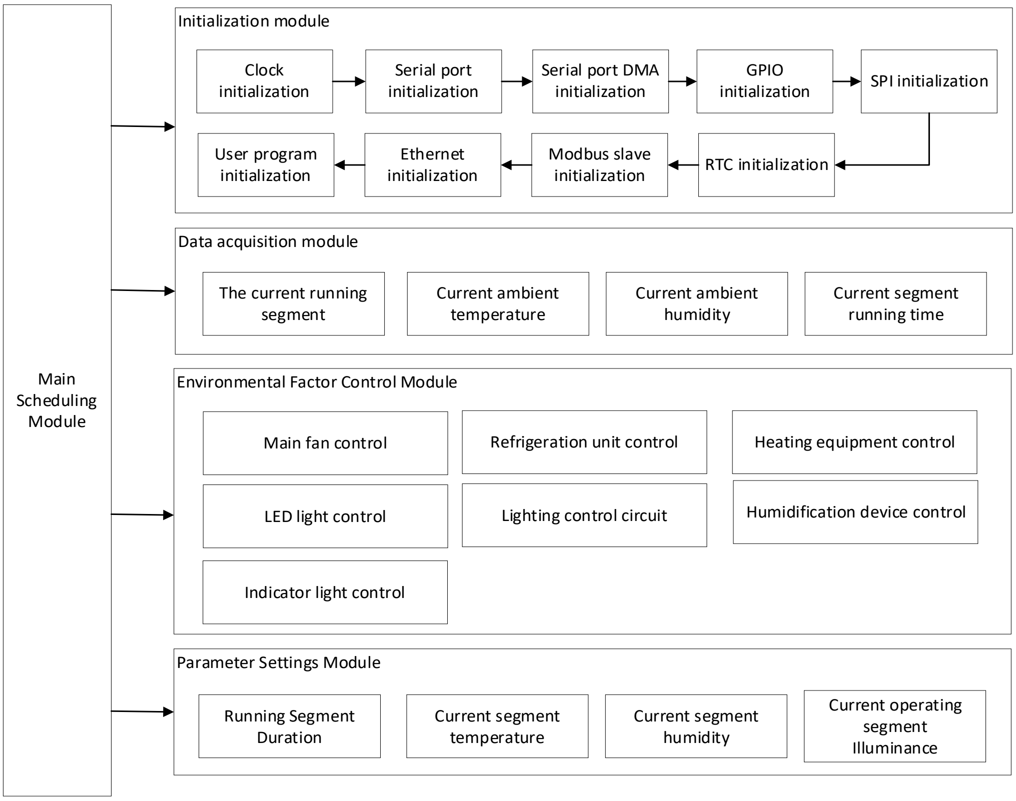

Figure 5. Software Overall Design Diagram

The main scheduling module is primarily used for coordinating various modules, establishing correct connections between each independent module to ensure proper execution of software modules and accurate data transmission. The software initialization module performs operations such as system clock initialization, serial port initialization, DMA initialization for serial ports, RTC clock initialization, SPI bus initialization, GPIO initialization, Modbus protocol stack initialization, Ethernet initialization, and user program initialization after the product is powered on, ensuring the correct execution of the software. The data acquisition module collects current temperature and humidity data inside the lithography machine chamber. The environmental factor control module is the core of the system, as its embedded temperature and humidity decoupling algorithm maintains a stable internal environment in the lithography machine chamber by controlling fans, auxiliary heating devices, cooling devices, humidification devices, and lighting equipment. The parameter setting module enables the configuration of required temperature, humidity, and illumination parameters inside the lithography machine chamber.

ISSN: 2472-3703 DOI: 10.6911/WSRJ.202511_11(11).0009

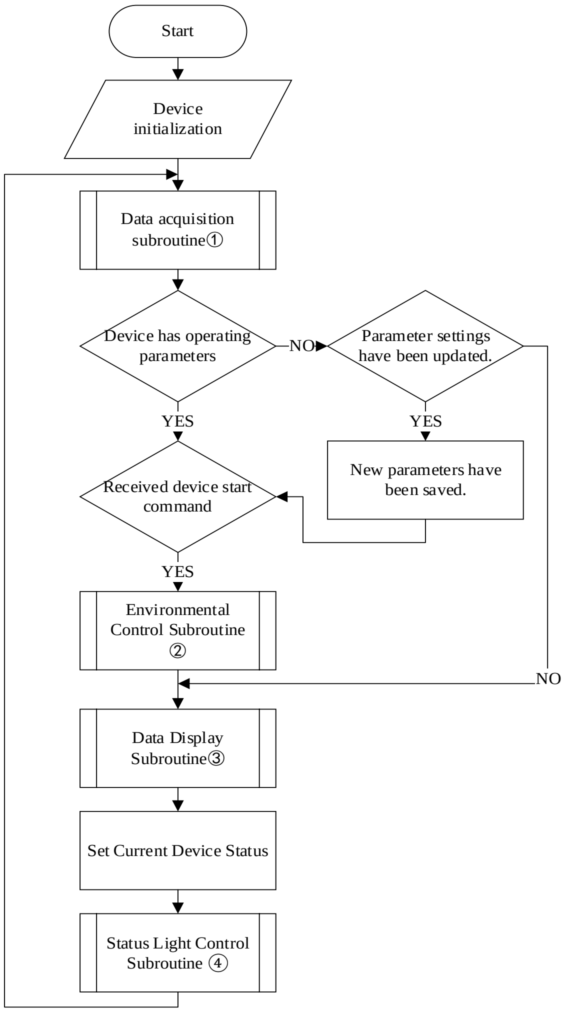

Figure 6. Software main flow chart

After completing the initialization of hardware and application software, the system enters the main loop. Within each cycle of the loop, it scans the keyboard and communication interface to check whether new parameters need to be configured; if so, the parameters are written into the system. Sensors periodically acquire temperature and humidity data inside the chamber, and the system adjusts the environment according to the set values. Finally, the real-time temperature and humidity are displayed on the screen, while the chamber's operating status is reported to the user terminal through the communication module. The detailed flow is shown in Figure 6.

5.3. System Implementation and Testing

To prevent the external environment from affecting the temperature and humidity inside the chamber, the system uses a sealed, thermally insulated enclosure. The system controller is mounted outside the thermal layer at the rear of the enclosure. The detailed flow is shown in Figure 7. Via the HMI, users can not only set the target temperature, humidity, illuminance, and run time for each segment, but also view real-time values for temperature, humidity, illuminance, remaining time of the current segment, and the operating status of the auxiliary heater, refrigeration unit, ventilation system, humidifier, and lighting system.

ISSN: 2472-3703 DOI: 10.6911/WSRJ.202511_11(11).0009

Figure 7. System hardware

To validate the functionality and performance of the environmental controller, the chamber was conditioned to 23 °C and 55 % RH. Temperature and humidity were recorded at 1-min intervals for 40 min. The temperature ranged from 23.0 °C to 23.13 °C, exhibiting a maximum fluctuation of 0.13 °C. Relative humidity varied between 54 % RH and 57 % RH, with a maximum deviation of 2% RH. Both parameters remained within the specified tolerances; the detailed data are presented in Figure. 8.

1	time	Temperature	humidity	time	Temperature	humidity	time	Temperature	humidity
2	10:21	23.13	56	10:31	23.04	56	10:41	23.13	56
3	10:22	22.91	57	10:32	23.04	57	10:42	23.1	57
4	10:23	23.11	55	10:33	23.02	54	10:43	23.12	55
5	10:24	22.98	55	10:34	23.01	56	10:44	23.07	55
6	10:25	22.92	54	10:35	22.94	57	10:45	22.98	56
7	10:26	22.89	53	10:36	22.92	55	10:46	22.93	54
8	10:27	23.01	56	10:37	22.98	55	10:47	23.01	54
9	10:28	23.04	57	10:38	23.01	57	10:48	23.04	55
.0	10:29	23.05	57	10:39	23.06	57	10:49	23.06	55
.1	10:30	23.02	56	10:40	23.08	56	10:50	23.01	56

Figure 8. Temperature & Humidity Test Data

6. CONCLUSION

The most critical environmental factors in a lithography machine chamber, temperature and humidity, are strongly coupled. An increase in temperature reduces humidity, while a decrease in temperature raises humidity. Conversely, an increase in humidity lowers temperature, and a decrease in humidity raises temperature. This study employs a decoupling algorithm to separate the control of temperature and humidity, resulting in satisfactory control performance after decoupling. However, the influence of LED cold lights on temperature and the residual heat from auxiliary heating equipment on the environment were not considered during the control process. If the residual heat from auxiliary heating equipment is recycled, it could effectively improve environmental control precision while reducing energy consumption.

ACKNOWLEDGMENT

Liaoning Institute of Science and Technology 2025 Undergraduate Innovation and Entrepreneurship Training Program (Project Number: 202511430107)

Liaoning Institute of Science and Technology 2026 Undergraduate Innovation and Entrepreneurship Training Program (Project Number: 202611430073)

2025 Liaoning Provincial Science and Technology Extension (Project Number: 210125018)

Pioneer Scientific Research and Innovation Team of Liaoning Institute of Science and Technology (Project Number: XKT202405)

REFERENCES

[1] Lan Z, Chen J, Xue C, et al. A temperature control algorithm for lithography machine based on generalized predictive control and BP neural network PI control [J]. Measurement and Control, 2024, 57(7):903-918. DOI:10.1177/00202940241226598.

ISSN: 2472-3703 DOI: 10.6911/WSRJ.202511_11(11).0009

[2] Mingsheng L, Jinrong W. Energy Performance Analysis of Coupled-Control Units With Both Thermostat and Humidistat [J]. Journal of Solar Energy Engineering, 2005, 127(1):65-69.

[3] Hu Y M, Fang L K. The Temperature and Humidity Control of Artificial Climate Chamber Based on Feed-Forward Compensation Decoupling [J]. Advanced Materials Research, 2013, 2708 (816-817):343-347.

[4] ZhouH, WuJ, ZhengX, et al. Fuzzy-PID controller based on improved LFPSO for temperature and humidity control in a CA ripening system [J]. Journal of Food Process Engineering, 2024, 47(6).

[5] Da G, Danfeng L, Yong Z, et al. Application of deep reinforcement learning to intelligent distributed humidity control system [J]. Applied Intelligence, 2022, 53(13):16724-16746.

[6] Jun D, Limin C, Gang C, et al. Design of adaptive humidity control system based on ultrasonic humidification in room temperature [J]. Journal of Physics: Conference Series, 2021, 1976(1).

[7] Zhang M, Jin L, Zhang J, et al. Analysis and Research on Coupling Characteristics of Temperature and Humidity Control System Based on Industrial Process [J]. Smart Systems and Green Energy, 2022, 4(1).

[8] Zhang M, Zhang J, Liu L, et al. Research on the Mechanism Model of Environmental Temperature and Humidity Control in Artificial Light Source Plant Factory [J]. Journal of Engineering Mechanics and Machinery, 2022, 7(2).

[9] Ganchev I, Taneva A, Kutryanski K, et al. Decoupling Fuzzy-Neural Temperature and Humidity Control in HVAC Systems [J]. IFAC PapersOnLine, 2019, 52(25).

[10] Paknahad M, Bachhal S J, Hoorfar M. Diffusion-based humidity control membrane for microfluidic-based gas detectors [J]. Analytica Chimica Acta, 2018, 1021103-112.

[11] Lan Z, Chen J, Xue C, et al. A temperature control algorithm for lithography machine based on generalized predictive control and BP neural network PI control [J]. Measurement and Control, 2024, 57(7):903-918.

[12] Lotfy K, Elshazly S I, Halouani B, et al. Wave propagation in nonlocal piezo-photo-hygrothermoelastic semiconductors subjected to heat and moisture flux [J]. Open Physics, 2025, 23(1):20250162-20250162.

[13] Wozniak L, Kalinowski P, Jasinski G, et al. FFT analysis of temperature modulated semiconductor gas sensor response for the prediction of ammonia concentration under humidity interference [J]. Microelectronics Reliability, 2018, 84163-169.

[14] Bhide A, Jagannath B, Graef E, et al. A Robust Electrochemical Humidity Sensor for the Detection of Relative Humidity Using Room Temperature Ionic Liquid (RTIL) for Integration in Semiconductor IC's [J]. ECS Journal of Solid State Science and Technology, 2018, 7(7):Q3043-Q3048.

[15] Moiz A S, Ahmed M M, Karimov S K. Effects of Temperature and Humidity on Electrical Properties of Organic Semiconductor Orange Dye Films Deposited from Solution [J]. Japanese Journal of Applied Physics, 2005, 44(3R):1199-1199.

[16] Rosty R, Kebbekus B, Zaitsev V. The testing of a semiconductor-based adsorption modified photosensitive sensor for its response to a volatile organic compound, oxygen, humidity and temperature [J]. Sensors & Actuators: B. Chemical, 2004, 107(1):347-352.